Construction and Building Materials 121 (2016) 120–133

Contents lists available at ScienceDirect

Construction and Building Materials

journal homepage: www.elsevier.com/locate/conbuildmat

Mechanical and durability evaluation of fiber-reinforced self-compacting concrete

Sherif Yehia *, AlaEddin Douba, Omar Abdullahi, Sharef Farrag

Department of Civil Engineering, American University of Sharjah, P.O. Box 26666, Sharjah, United Arab Emirates

HIGHLIGHTS

- Effect of fiber addition on mechanical and durability characteristics of SCC was evaluated.
- Effect of early wetting/drying cycles on FRSCC mechanical properties was investigated.
- Microstructural analysis of FRSCC and correlation with macro-properties was conducted.
- Low chloride permeability was achieved confirming adequate durability of FRSCC.

ARTICLE INFO

Article history:
Received 5 May 2014
Received in revised form 27 March 2015
Accepted 22 May 2016

Keywords:
Self-compacting concrete
SCC
Fiber reinforced SCC
Synthetic fiber
Steel fiber
Hybrid fiber
Mechanical properties

ABSTRACT

In this paper, an investigation of the mechanical properties and durability aspects of steel, synthetic, and hybrid fiber-reinforced self-compacting concrete exposed to early wet/dry cycles are presented and discussed. The experimental program consisted of two phases. Phase I involved tests on specimens for workability, mechanical properties, Rapid Chloride Penetration (RCP), and Scanning Electron Microscopy (SEM). The evaluation of mechanical properties included compressive, flexural and splitting tensile strengths, and modulus of elasticity. In Phase II, specimens were exposed to wet/dry cycles, and the effect of moisture on mechanical properties was investigated. All mixes in Phase I achieved a cube compressive strength of 70 ± 5 MPa. Furthermore, it was observed that exposure of Fiber-Reinforced Self-Compacting Concrete (FRSCC) to early wet/dry cycles improved the mechanical properties of all mixes; an increase in compressive strength of 10 MPa compared to non-exposed specimens was observed. The microstructure of Synthetic Fiber-Reinforced Self-Compacting Concrete (SyFRSCC) and Steel Fiber-Reinforced Self-Compacting Concrete (SFRSCC) was different, which explains the difference in their respective crack-resistance mechanisms.

1. Introduction

Self-compacting concrete (SCC) is characterised by its ability to consolidate under its own weight without any means of compaction or vibration. SCC has the ability to spread smoothly in congested reinforced elements due to its flowability and use of small size aggregates [1–3]. SCC has been used in several projects including residential buildings or large infrastructure for densely reinforced elements such as walls, load transfer floors, precast elements, and offshore structures and for many other [2,4–6]. In addition, SCC generally reduces casting time, labour, and equipment needed [5,7]. However, the resistance of SCC to environmental conditions and cracking resistance are not similar to that of ordinary concrete (OC) [8].

Introducing fibers into the concrete matrix can improve its properties, and enable the utilization of high strength concrete, while maintaining a ductile behaviour. Self-compaction encourages the application of macro-fiber reinforcement in concrete, mitigating concerns regarding reduced workability [9,10]. Steel or synthetic fibers help to improve various mechanical properties, fire resistance and reduce plastic shrinkage of SCC as well as to enhance the sustainability of a SCC matrix [3,11–15].

In this paper, the effect of synthetic, steel, and hybrid fibers addition on the mechanical properties and durability aspects of SCC under exposure to wet/dry cycles starting at day 7 after casting was evaluated. Testing was conducted in two phases; in Phase I, samples were kept in laboratory conditions and tested for compressive, flexural and splitting tensile strengths, and modulus of elasticity. While in Phase II, the mechanical properties were evalu-

* Corresponding author.
E-mail addresses: syehia@aus.edu (S. Yehia), b00035697@gmail.com (A. Douba), b00037324@aus.edu (O. Abdullahi), sfarrag@alumni.aus.edu (S. Farrag).

http://dx.doi.org/10.1016/j.conbuildmat.2016.05.127
0950-0618/

ated after subjecting the samples to wetting and drying cycles for 21 days.

2. Background

Several fresh and hardened state properties are important to describe the behaviour of FRSCC. It is commonly known that fibers tend to negatively impact the workability of SCC. The magnitude of this impact is related to the fibers' type, geometry, volumetric ratio, and dispersion in the concrete [16]. Equally important is the effect on the mechanical properties due to the presence of fibers. Moreover, the durability of SCC can be improved by the presence of fibers as results of various tests suggest [17].

Exposure to early wetting and drying cycles might improve hydration and lead to enhanced mechanical properties, which highlights the importance of curing. Moreover, there is a contradiction about the effect of fibers in SCC. This is mainly due to a variation of fiber distribution and volume percentage, variation in SCC mixes, and the tested samples' shape and size [1,3,18–21]. Some manufacturers suggest optimal fiber dosages for specific products, but the variation in mix design used in production can still cause variation in performance. As for fiber distribution, steel fiber dispensed into the matrix might be controlled by magnetic fields, which is not possible for synthetic fibers [22]. Furthermore, a proper fiber distribution provides better crack control to achieve improved durability and enhanced mechanical properties [8,23]. Fig. 1 shows the variation in mixture proportions by depicting SCC and FRSCC mixes [1,8,14,24–26]. Cement and water contents are within a limited range. Yet, it is observed that the main variables among all mixes are the fine and coarse aggregate contents. This can be explained by the variation of mixing procedures available to produce SCC, presented in [27]. All mixes contained superplasticizers to improve workability and to reduce the negative effect of fibers on workability. Fillers such as Ground-granulated Blast Slag (GGBS), fly ash, silica fume, and limestone powder dosages varied with the deviation of target compressive strength and availability. Typically, FRSCC mixes have coarse aggregate volume fractions of 20–50%, while the fine aggregate contents can be in the range of 20–60%. The aggregate content can vary based on strength, density, and durability requirements. Cementitious materials are usually within 10–30% of concrete volume, and water content is within 5–20%. Steel fiber content is typically capped at 2 Vol.-% to avoid significant effect on workability. On the other hand, <1 Vol.-% is recommended for applications with synthetic fibers [25,26]. As for hybrid-reinforced SCC, the volumetric fraction can vary based on the synthetic-to-steel fiber ratio.

2.1. Effect of fibers on SCC properties

2.1.1. Fresh stage properties

In general, the addition of fibers to concrete will reduce the flowability/workability of SCC concrete [1,14,15,28]. Although the fiber length can have a remarkable effect on workability, steel fibers reduce the workability of SCC more than polypropylene fibers because of their configuration and their higher stiffness at same fiber length, increasing the friction between the fibers and the aggregates [29]. In addition, the fibers' shape (twisted, hooked, deformed, etc.) can further contribute to workability loss. If steel fibers are not well distributed, clumping of fibers might occur, which can ultimately affect mechanical properties as well as workability [3,13,14]. On the other hand, although synthetic fibers do not impose such difficulties, balling of synthetic fibers can reduce workability if they are not well-distributed during batching [26,30–33]. It is recommended to avoid rapid addition of fibers during mixing.

2.1.2. Hardened stage properties

Mechanical properties of SCC can be enhanced by the addition of fibers; the performance of fiber-reinforced concrete is generally compared to fiber-free concrete. This is due to the initiation and rapid propagation of cracks in fiber-free concrete, which will reduce the stiffness and load resistance ability [5,15,34]. In addition, fiber reinforcement can shift the behaviour of SCC from strain-softening to strain-hardening or pseudo strain-hardening, enhancing the post-cracking performance and ductile behaviour [16]. Table 1 summarizes the effect of the addition of steel, synthetic, and hybrid mix fibers on various properties of SCC.

2.1.3. Microstructure

Less emphasis was directed towards investigating the microstructural features of FRSCC as opposed to mechanical, work-

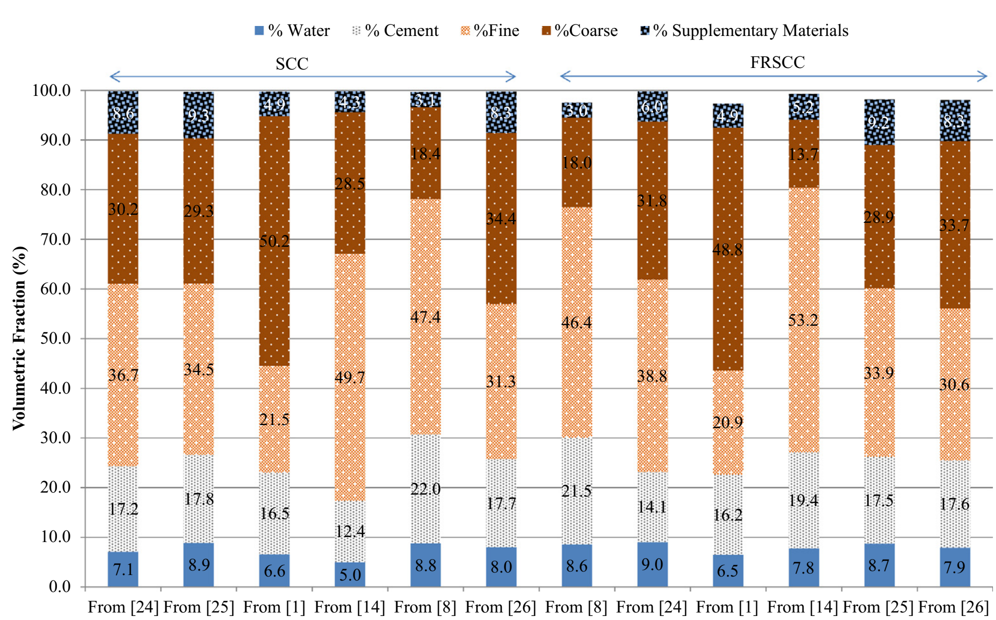

Fig. 1. Example of SCC and FRSCC mixtures obtained from available literature.

Table 1
Enhanced performance due to the addition of fibers as opposed to fiber-free SCC.

Property	FRSCC Mix		
	SFRSCC	SyFRSCC	HyFRSCC
Compressive Strength	Steel fibers cause a delay in the propagation of macro cracks, allowing concrete to attain higher peak stresses	Synthetic fibers help restrain the formation of micro cracks, reducing loss of stiffness and allowing for higher load transfer	Combination of both fibers help produce concrete that resist macro and micro cracks
	Steel and synthetic fibers bridge cracks leading to a higher resistance to compressive loads and to an improved post-cracking behaviour. However, it is generally reported that fiber reinforcement does not have an effect on the compressive strength [38,14,25,34,35]. Nevertheless, a high dosage of fibers can result in a pronounced reduction in compressive strength due to a high concentration of fibers in some sections of a concrete element [14]		
Flexural Strength	Steel fibers are produced with different shapes and have different bonding abilities with the concrete. At a high tensile stress, the high tensile strength of fibers helps to resist more loads from surrounding concrete	Synthetic fibers are deformable with low unit weight that allows the fibers to have a uniform distribution providing various flexural stress resisting planes	Having both fibers within the matrix will allow adequate fibers orientation as well as high bonding strength. Therefore, HyFRSCC can provide the highest increase in flexural strength [36,37]
	Synthetic and steel fibers help to improve the flexural strength of FRSCC and provide a higher modulus of rupture [3,14,34]. However, a uniform Fiber distribution within the concrete element is needed to achieve the optimum flexural strength [22,34]		
Splitting Tensile Strength	Synthetic and steel fibers tend to increase the tensile strength of a concrete element [3,14,34,35]. Nevertheless, it should be noted that excessive dosages of fibers might result in increasing air voids which can adversely affect concrete and lead to a decreased tensile strength capacity [8]		
Modulus of Elasticity	Due to steel fibers' configuration, higher strain can be attained due to their high modulus of elasticity. At optimum fibers dosage, steel fibers can help the element to withstand higher deformation at peak stresses	Synthetic fibers can improve the resistance to deflection up to 90% for concrete beams while also suggesting a positive correlation between the percentage of fibers and the resistance to deflection in long and short beams [13]	HyFRSCC mixes reported an increase in modulus of elasticity as both fibers help providing improved cracking mechanism and distribute the load over the element to attain higher strains [23]
	FRSCC elements can show less strain at peak stress compared to fiber-free SCC [26]. In general, the addition of fibers will lead to an increase in modulus of elasticity and an improved ductile behaviour of SCC [1,14,23]		
Crack Control	Synthetic fibers help in restraining the formation of micro-cracks within a cross-section because of their high dispersion [8,13,17,38]	Steel fibers significantly enhance the resistance to tensile stresses causing a better crack distribution. They delay the propagation of macro-cracks, if properly distributed and oriented in a matrix is achieved [6,14,39–41]	The presence of both fibers in a hybrid composite system can result in an enhanced cracking control as micro and macro cracks will be restrained. An increase of post-cracking load resistance has been reported [38]
	In general, if the same fiber amount crosses a crack-propagation plane, steel fibers provide more resistance and better bridging than synthetic fibers [29]		
Microstructural Features	Differences in stiffness of constituents in concrete can greatly affect the paste/aggregate interface, introducing cracks and weakening the interaction [42]. This can be more significant in the case of a fiber addition to concrete; steel fibers are substantially stiffer than the cement paste		

ability, durability, and structural application aspects. Furthermore, mechanical properties were studied including the micro-structure and paste/aggregate interaction. In addition, it is important to ensure adequate strength of the Interfacial Transition Zone (ITZ) between different concrete constituents. Table 1 provides information on the effects of different fibers on the microstructure of SCC.

2.2. Durability

Although durability does not have a single quantitative measure, there are several means that aid in assessing concrete quality concerning durability such as water absorption, depth of water penetration, water permeability, chloride permeability, sodium sulphate permeability, magnesium sulphate permeability, capillary absorption coefficient, and carbonation resistance [5,39,43]. In addition, subjecting concrete specimens to wet-dry cycles and temperature variation can provide an indication of concrete performance [43]. Results found in the literature suggest better performance of SCC than that of conventional concrete in terms of rapid chloride permeability test (RCPT) [39,43]. Furthermore, the presence of fibers can help to improve crack control by bridging between cracks hence reducing concrete's permeability.

3. Experimental program

The three objectives of the experimental investigation were to 1) evaluate the mechanical properties of SCC reinforced with steel, synthetic, and hybrid fibers, 2) investigate the effect of early age wet/dry cycles exposure on the mechanical properties of SCC reinforced with steel, synthetic, and hybrid fibers, and 3) examine durability-related aspects of FRSCC by conducting the Rapid Chloride Penetration (RCP) test, and Scanning Electron Microscopy (SEM). To achieve these goals, the experimental program was divided into two testing phases. For the first phase, samples were kept at laboratory conditions (~25 °C and 75% RH) and tested for compressive strength, splitting tensile and flexural strength, modulus of elasticity, RCP, and SEM scans. In Phase II of testing, the mechanical properties were evaluated after subjecting the samples to wetting and drying cycles. It is known that 3 days of curing is required as a minimum, while 7 days is a recommended duration to ensure better hydration [44]. The curing technique implemented in the current study simulates curing conditions, where concrete is cured at a time and then left to dry until the next cycle.

3.1. Casting

A standard procedure was followed during mixing to achieve the target flowability before adding the fibers. The fibers were added gradually in order to avoid balling and to attain a uniform distribution within the mix. The slump flow test was used to measure the self-compaction ability for all four mixes. In addition, the sieve stability, J-ring, and orimet tests were conducted to assess the segregation resistance, passing ability, and filling ability of the mixes [45]. All samples in both phases were demoulded after 24 h while moist curing continued for 3 days.

3.2. Wetting and drying cycles

This procedure was followed for samples in the second phase. Between, the 3rd and 7th day, all samples were left to air dry in laboratory conditions. Then, specimens were exposed to continuous wet-dry cycles. The specimens were submerged in water for 24 h and then they were exposed to the summer climate of the UAE for 24 h. The maximum humidity and temperature values are shown in Fig. 2. After 21 days of the wetting-drying cycles (28 days after casting), the mechanical properties were evaluated according to specifications. Tap water with pH = 7.8, Total Dissolved Solids (TDS) in the range of 700–800 ppm, and chloride content <0.05 ppm was used for wetting of specimens. Water salinity did not interfere with the exposure.

3.3. Testing program

Table 2 summarizes the tests, numbers of samples, sample size, and standards followed during testing [46–51]. For each testing event, at least two samples were tested from each FRSCC mix as well as the control mix. Compressive strengths reported in the current study are cube strengths. However, cylindrical specimens were prepared to use the compressive strength results for different ACI prediction

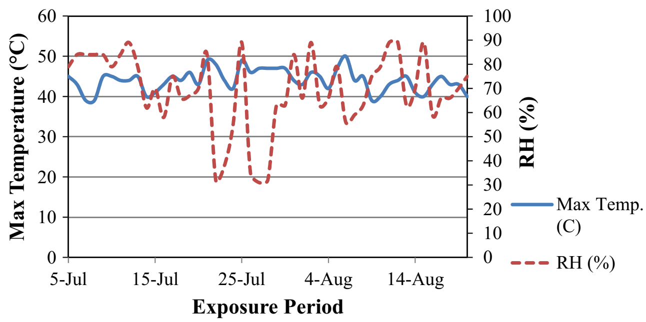

Fig. 2. Temperature and humidity variation during exposure period.

Table 2
Summary of the experimental program.

Test	Specification	Number of Samples tested from each mix	Sample Size (mm)	Testing at
Compressive Strength	BS EN 12390-3 [46]	2 Cubes	150 × 150 × 150	3, 7, 21 and 28 days after casting
	ASTM C39 [47]	2 Cylinders	150 × 300	3, 7 and 28 days after casting
Splitting Tensile Strength	ASTM C496 [48]	2 Cylinders	100 × 200	28 days after casting
Flexural Strength	ASTM C78 [49]	2 Beams	100 × 100 × 500	3, 7, 21 and 28 days after casting
Modulus of Elasticity	ASTM C469 [50]	2 Cylinders	150 × 300	28 days after casting
Rapid Chloride Permeability Test	ASTM C1202 [51]	2 Cylinders	100 × 50	90 days after casting

equations. Additional samples were prepared to conduct the RCPT and SEM scans. The RCPT samples (50 mm thick with a diameter of 100 mm) were saw-cut from the middle of concrete cylinders. A special procedure was followed for the SEM samples preparation to avoid micro-cracks.

3.4. Materials

Coarse aggregate (crushed limestone) having maximum size of 10 mm was used for all mixtures. Crushed sand (1–4.75 mm) and dune sand (<0.3 mm) were used as fine aggregate. The total volumetric content of the fine aggregate was split equally between the crushed and dune sand. Crushed aggregates were angular and rough, while dune sand was round and smooth. Dune sand was added to enhance the workability of the mix, while maintaining an adequate fine aggregate size distribution by including the crushed sand, in order to ensure a dense mix. Silica fume was added to the mix to provide viscosity, increase strength, and act as a filler to improve the bond between the particles. A commercially available superplasticiser (BASF Glenium Sky 504) was used to achieve flowability. The steel fibers had an aspect ratio of 67 and a length of 50 mm (Modulus of Elasticity = 210 GPa, Tensile Strength = 1000 MPa) [52], whereas synthetic fibers (Modulus of Elasticity = 9.5 GPa, Tensile Strength = 620 MPa) had an aspect ratio of 90 and length of 40 mm [53]. Physical and mechanical properties of the aggregates were tested according to specifications [54–59] in order to ensure the quality of the mixes produced using local materials in the United Arab Emirates. Results of such tests are shown in Table 3. The coarse aggregates were neither elongated nor flaky, which implies that aggregate shape would not have a pronounced impact on workability. In addition, the Aggregate Crushing Value (ACV) and Los Angeles Abrasion (LAA) value were less than 25%, indicating adequate crushing of aggregates under applied load. Table 4 presents the control (SCC), synthetic (SyFRSCC), steel (SFRSCC), and hybrid reinforced self-compacting concrete (HyFRSCC) mixes, that were used in both phases of the experimental program. It also shows typical volumetric fractions of each constituent in FRSCC. The control mix shown in Table 4 was developed by [27] based on the absolute volumetric method with a target strength of 70 MPa. All mixes had a water-to-cement ratio of 0.45 and water-to-binder ratio (cement and silica) of 0.36. Nevertheless, minor adjustments with regard to the crushed sand content were applied to account for the fiber dosage while keeping the w/b ratio the same in order to have comparable workability/self-compaction performance among all mixes. In all FRSCC mixes, 0.5 Vol.-% (as replacement of crushed sand) fiber dosage was maintained; the hybrid mix contained 0.25 Vol.-% of each fiber type. The recommended dosage of the superplasticizer used is 800–1500 ml/100 kg of cement.

4. Experimental results

4.1. Fresh stage properties

The effect of fibers on workability was evaluated by using the same superplasticiser dosage for all mixes. Table 5 summarizes the results of the fresh stage evaluation. The slump flow for each mix was measured immediately after concrete mixing. Fig. 3 illustrates the slump flow achieved for the different mixes; all mixes reached a satisfactory level of flowability. Furthermore, all mixes generally met the criteria with regards to filling ability and segregation resistance requirements. However, SyFRSCC and HyFRSCC particularly exhibited a lower passing ability as indicated from the J-ring test.

4.2. Hardened stage properties

Mechanical properties evaluation for Phases I and II followed the testing program presented in Table 2. Results of the mechanical properties evaluation are summarized in Table 6. For testing events in which the difference between the results of two samples was >5 MPa, the sample was rejected. In addition, results from the following test events were used to monitor the strength development and determine if the variation was limited due to sample preparations. Such scatter in data could be experienced due to the fiber distribution among the samples and the samples preparation.

Compressive strength: For all mixes in Phase I, the target cube strength of 70 ± 5 MPa was reached with the SyFRSCC mix providing higher strength than that of the control mix at 28 days. Whereas for Phase II, the cube compressive strengths of the mixes were 80 ± 5 MPa, indicating an overall strength increase of the wet/dry cycles-exposed specimens compared to the unexposed one. In order to show failure due to compression testing, Fig. 4 depicts representative samples of each mix after failure. Control mix specimens failed in an explosive manner due to crushing while FRSCC mixes failed with an enhanced post-cracking performance.

Flexural strength: The presence of the fibers increases the flexural strength. However, since fiber type has a different mechanism of restraining cracks and resisting internal tensile stresses, each FRSCC mix tends to perform differently in flexural testing, as is shown in Table 6. Among all tests, FRSCC mixes performed better than the control mix in both phases. The addition of fibers led to an increased SCC flexural strength in both phases in the range of 7%–55%. The SyFRSCC mix achieved a similar flexural performance in both phases, with an increase of 26% and 45% compared to the control specimens in Phases I and II respectively. Fig. 5a and b show the distribution of fibers of tested SFRSCC and SyFRSCC samples respectively. It can be observed that the fibers are well-distributed over the depth of the prism, which confirms that a homogeneuos fiber distribution was achieved. While all tested samples failed satisfactorily in flexure, the control mix specimens were split in half with sudden failure, as shown in Fig. 4. However, because of the fibers' ability to bridge cracks, resisting tensile forces, and to improve the ductility of concrete, all FRSCC samples showed improved post-cracking behaviour as demonstrated in Fig. 4.

Splitting tensile strength: Although the flexural strength is an indicator of the tensile strength, the splitting tensile strength also can confirm such findings since it indirectly measures the tensile strength. Results shown in Table 6 clearly indicate an increase in the splitting tensile strength after the addition of fibers for all fiber mixes compared to the control mix in both phases. Moreover, the control mix in Phase II showed a noticeable increase (0.5 MPa) in splitting tensile strength due to the improved hydration. The SyFRSCC mix presented the lowest increase in tensile strength while it provided the highest rise in flexural strength. Hairline crack is shown in Fig. 4 as indication of failure of SFSCC samples in this test.

Modulus of elasticity: The modulus of elasticity is related to stiffness of concrete. However, the stress-strain diagram can be used to indicate ductile behaviour of concrete. The results of modulus of elasticity achieved in Phases I and II are shown in Table 6. Almost all samples containing fibers achieved a small increase in moduli in the range of 6–13% relative to the control mix. Nevertheless, steel fibers led to a higher increase of modulus of elasticity by examining the overall increase from SFRSCC in Phase I and HyFRSCC in Phase II.

Table 3
Properties of aggregates used in the current study.

	Physical								Mechanical	
	Flakiness Index (%)	Elongation Index (%)	Bulk Density (kg/m^3)		Absorption (%)	Bulk Dry Specific Gravity	Bulk Specific Gravity	Apparent Specific Gravity	ACV* (%)	LAA** (%)
			Loose	Compacted						
Coarse Aggregate	15	8.7	1412	1513	1.1	2.62	2.65	2.7	20	18
Fine Aggregate (Crushed sand)	–	–	1394	1729	2.3	2.51	2.57	2.66	–	–
Fine Aggregate (Dune sand)	–	–	1295	1620	1.0	2.56	2.58	2.63	–	–
Limit	<25	<15	–	–	–	–	–	–	<23	–
Standard Used	BS 933-3:2012 [54]	BS 812:105.2 [55]	ASTM C29/C29M [56]		ASTM C127 [57]				BS EN 1097-2:2010 [58]	ASTM C 131-06 [59]

* Aggregate Crushing Value.
** Los Angeles Abrasion Score.

Table 4
SCC, SyFRSCC, SFRSCC, and HyFRSCC concrete mix constituents.

Constituent	Specific Gravity	Mix				
		Typical Volumetric Fraction Range	SCC (kg/m^3)	SFRSCC (kg/m^3)	SyFRSCC (kg/m^3)	HyFRSCC (kg/m^3)
Cement	3.15	0.1–0.2	409.5	409.5	409.5	409.5
Silica Fume	2.20	0–0.08	110.0	110.0	110.0	110.0
Water	1.00	0.05–0.2	185.0	185.0	185.0	185.0
NW CA	2.56	0.2–0.5	793.6	793.6	793.6	793.6
Coarse Sand	2.58	0.2–0.6	374.1	361.2	361.2	361.2
Dune sand	2.58		464.4	464.4	464.4	464.4
Synthetic Fiber	0.92	0.025–0.05	–	–	4.6	2.3
Steel Fiber	7.77		–	38.8	–	19.4
Superplasticizer	1.11	0–0.01	7.0	7.0	7.0	7.0

Table 5
Fresh stage evaluation results.

	Slump Flow		J-ring		Sieve Stability	Orimet
	Spread (mm)	T50 (sec)	B_j* (cm)	$T50_j$ (s)	% Passing	T_O (s)
Control	770	4.2	0.9	5.7	22.0	1.3
SyFRSCC	700	8.1	6.0	38.1	15.3	2.5
SFRSCC	700	14.5	1.4	21.5	13.3	1.9
HyFRSCC	630	7.9	2.6	26.0	12.7	2.9

* Blocking step (height difference between concrete center and concrete edge).

4.3. Rapid chloride penetration test (RCPT)

The RCPT provides information about concrete resistance to chloride ion penetration, indication of concrete density and how permeable concrete is [44]. The results, reported in Coulombs, should not to be interpreted quantitatively, but rather qualitatively. All mixes had a very low chloride penetration potential determined according to ASTM C1202 is as shown in Table 7, which indicates that all mixes have a low permeability and are dense. This indicates very low likelihood of deterioration due to chloride penetration.

4.4. Scanning Electron Microscopy (SEM)

The goal of the SEM images was to study the interaction between fibers and surrounding mortar at the microstructural level in an attempt to explain macro-behaviour. No samples were extracted from HyFRSCC due to the difficulty of obtaining a sample containing both fibers.

4.4.1. Cement paste

Fig. 6(a) shows the morphology of the cement paste. Particles prevalently manifested as irregular poorly-crystalline formations, indicating Calcium-Silicate-Hydrate (C-S-H), the primary result of cement hydration. The particles varied in size, with the largest dimension ranging between 0.5 and 4.53 μm. Moreover, energy dispersive X-ray spectroscopy results displayed in Fig. 6(b) showed high concentrations of Al (35.7%), Si (32.5%), and Ca (14.3%), confirming that the formations are C-S-H particles.

4.4.2. Steel fiber-cement paste interaction

The interaction between steel fibers and mortar was the focus for SFRSCC samples. Fig. 7a depicts a magnified steel fiber. It shows the innate surface roughness of the steel fibers due to the manufacturing process, resulting in parallel longitudinal grain lines. Fig. 7(b) illustrates a 40× magnified image of a steel fiber surrounded by mortar from the indicated location. There was no space observed between the fiber and the surrounding paste. In addition, there were no visible cracks at this magnification level. Equally important, a distinct black layer surrounding the entire perimeter of the steel fiber (wall effect) was observed. However, its thickness could not be estimated at this magnification level. Fig. 7(c) and (d) present 390× and 500× magnified images respectively which helped in identifying this layer. The thickness of the layer was estimated from the latter which was approximately 8.5 μm. The image was further magnified up to 1120× and micro-cracks were clearly visible as is displayed in Fig. 7(e). The average estimated crack width was ~0.5 μm.

4.4.3. Synthetic fiber-cement paste interaction

Fig. 8(a) shows the smooth surface of a synthetic fiber filament. Fig. 8(b) illustrates a ~40× magnified image with the indicated location of both different lateral and longitudinal cross-sections of the fiber. This in turn depicts arbitrary geometric configuration of the fibers because of their distribution in the matrix. It shows the interface between both filaments and the surrounding cement paste, and the existence of some hairline cracks. It can be observed from Fig. 8(c) and (d) that there is noticeable constricted mechanical interlock. In addition, more cracks were clearly visible at a 1000× magnification compared to SFRSCC, and their average width was ~0.4 μm. Similarly, cracks were propagating radially rather than along the fibers, confirming a good bond between fibers and cement paste. Moreover, there was no wall-effect observed around synthetic fiber filaments as opposed to steel fibers, as is illustrated in Fig. 8(d).

5. Discussion

5.1. Fresh stage and mechanical properties

Various effects of fiber addition were observed on the fresh stage properties of SCC at the fiber dosage applied in the current study (0.5 Vol.-%). Regardless of fiber type, all mixes had a slump

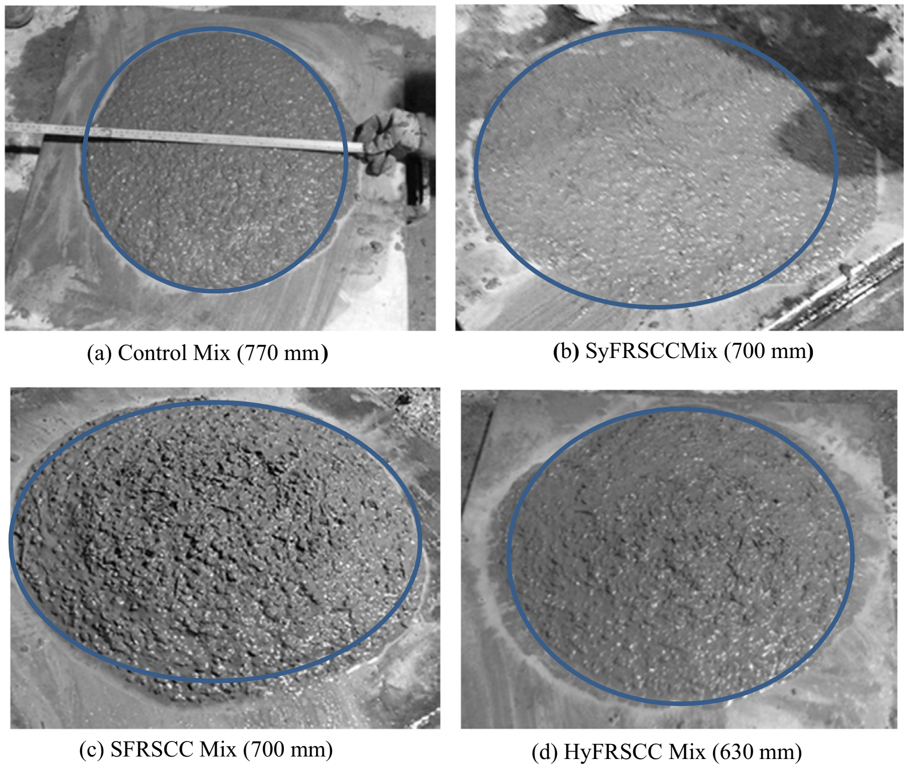

Fig. 3. Slump flow achieved by different FRSCC mixes.

Table 6
Results of mechanical properties evaluation.

	Mix	Cube Compressive Strength – $f'c_c$ (MPa)				Cylinder Compressive Strength – $f'c_{cy}$ (MPa)			Flexural Strength – f_r (MPa)				Splitting Tensile Strength – f_s (MPa)	Modulus of Elasticity – E (GPa)
		Age (Days)												
		3	7	21	28	3	7	28	3	7	21	28	28	28
Phase I	Sample 1	*42.8*	*54.6*	*74.1*	*70.4*	~~*24.6*~~	~~*37.7*~~	*58.3*	*4.30*	*4.55*	*5.10*	*6.25*	*3.45*	*24.5*
	Sample 2	*46.8*	*55.1*	*75.5*	*73.7*	*34.6*	*53.2*	*60.5*	*4.55*	*5.05*	*5.70*	*6.60*	*4.08*	*28.6*
	Control	**44.8**	**54.9**	**74.8**	**72.1**	**34.6**	**53.2**	**59.4**	**4.43**	**4.80**	**5.40**	**6.43**	**3.77**	**26.6**
	Sample 1	*35.5*	*46.0*	*63.1*	*69.2*	*29.2*	*26.4*	*59.2*	*5.30*	*5.10*	*6.23*	*8.20*	*4.06*	*26.2*
	Sample 2	*35.8*	*48.9*	*64.4*	*81.2*	*29.4*	*38.1*	*62.6*	*5.60*	*5.40*	*6.58*	*8.28*	*4.14*	*27.5*
	SyFRSCC	**36.2**	**47.5**	**63.8**	**75.1**	**29.3**	**32.3**	**61.3**	**5.45**	**5.25**	**6.41**	**8.24**	**4.10**	**26.8**
	Sample 1	*42.9*	*55.4*	*67.7*	*70.6*	*34.9*	~~*29.4*~~	*63.8*	*5.35*	*6.50*	*6.95*	*6.90*	*4.47*	*26.6*
	Sample 2	*43.3*	*57.3*	*71.7*	*72.1*	*36.0*	*56.0*	*66.2*	*6.40*	*7.30*	*8.05*	*7.10*	*5.08*	*29.9*
	SFRSCC	**43.1**	**56.4**	**69.7**	**71.4**	**35.5**	**56.0**	**65.0**	**5.88**	**6.90**	**7.50**	**7.00**	**4.78**	**28.3**
	Sample 1	*43.7*	*56.1*	*70.5*	*69.2*	*39.7*	*56.2*	*63.6*	*6.55*	*6.10*	*7.40*	~~*5.50*~~	*6.35*	*25.8*
	Sample 2	*45.1*	*58.6*	*72.2*	*69.6*	*45.0*	*57.2*	*64.9*	*7.75*	*6.25*	*7.90*	*7.90*	*7.13*	*29.2*
	HyFRSCC	**44.4**	**57.4**	**71.4**	**69.4**	**42.4**	**56.7**	**64.3**	**7.15**	**6.18**	**7.65**	**7.90**	**6.74**	**27.7**
Phase II	Sample 1				*80.6*							*6.00*	*4.40*	*28.7*
	Sample 2				*81.1*							~~*3.10*~~		*29.7*
	Control	–	–	–	**80.9**	–	–	–	–	–	–	**6.0**	**4.40**	**29.2**
	Sample 1				*73.8*							*7.80*	*3.70*	*31.0*
	Sample 2				*80.6*							*9.60*	*4.45*	~~*44.8*~~
	SyFRSCC	–	–	–	**77.2**	–	–	–	–	–	–	**8.70**	**4.5**	**31.0**
	Sample 1				*72.0*							*6.95*	*3.60*	*33.2*
	Sample 2				*89.7*							*9.15*	*6.00*	~~*37.4*~~
	SFRSCC	–	–	–	**80.9**	–	–	–	–	–	–	**8.05**	**4.8**	**33.2**
	Sample 1				*79.2*							*9.2*	*6.18*	*31.1*
	Sample 2				*80.8*							*9.45*	*6.77*	*27.2*
	HyFRSCC	–	–	–	**79.7**	–	–	–	–	–	–	**9.33**	**6.48**	**29.2**

Strike through indicate that these results are not acceptable and further monitoring is required.

flow in the range of 600–770 mm within 4–15 s. Although the slump flow is a relatively rapid and easy test to conduct, other tests can better serve judging segregation resistance, passing ability, and filling ability of SCC. The J-ring, a reasonable representation of site conditions, was conducted in the current study, and fiber addition exhibited an effect on the passing ability. Synthetic fibers addition substantially reduced the passing ability of SCC by increasing B_j from 0.9 cm to 6 cm and 2.6 cm in SyFRSCC and HyFRSCC, respectively, whereas SFRSCC achieved a B_j of 1.4 cm. B_j is defined as blocking step (height difference between concrete center and con-

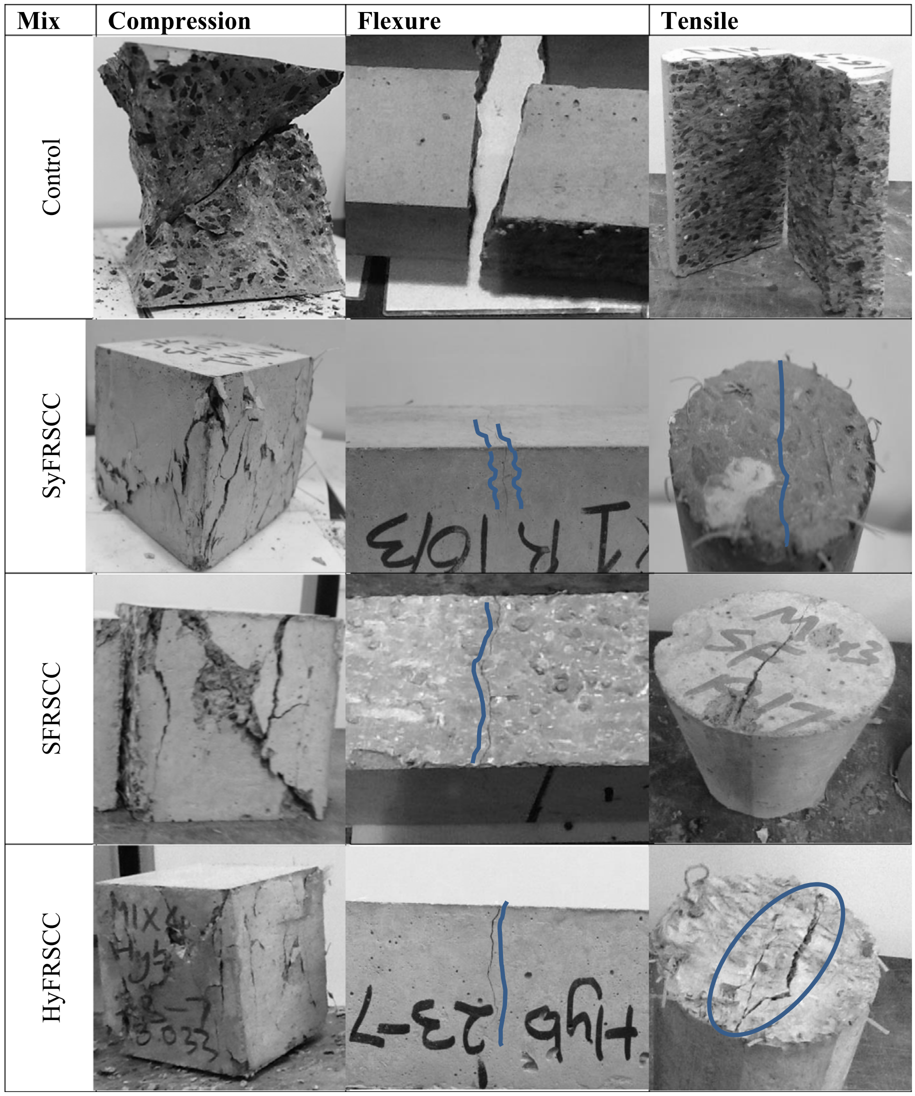

Fig. 4. Failure modes of the concrete mixes under various loading.

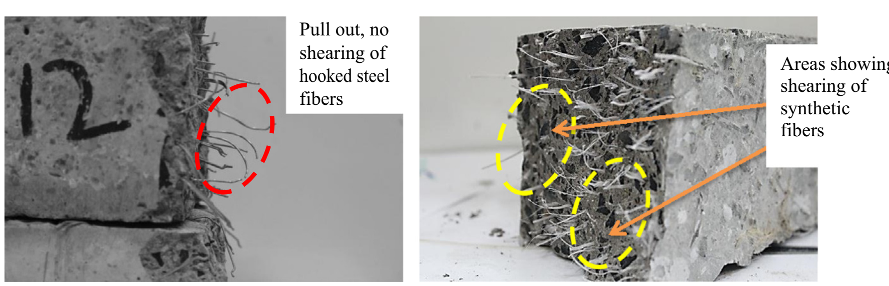

(a) SFRSCC (b) SyFRSCC

Fig. 5. Fiber distribution in FRSCC mixes.

crete edge) and typically a maximum of 1.5 cm height difference is considered for plain SCC. This could be attributed to the higher surface area and aspect ratio of synthetic fibers at same fiber volumetric content and similar length compared to steel fibers. This was also observed in the hybrid mix, in which the B_j was in between the two mixes SFRSCC and SyFRSCC. Similar findings were reported in [9,62,63] that steel fiber does not affect self-compaction features as opposed to the other fiber in a hybrid system. Furthermore, fiber addition increases the viscosity of concrete which enhances the segregation resistance. In addition, the flow time needed to reach 500 mm significantly increased when the J-ring was used as is shown in Table 5. The filling ability of SCC was not affected by fiber addition comparing the results of the orimet test obtained from the different mixes, for which falling durations >5 s are considered to be significant. Equally important, the fiber addition increased the segregation resistance of concrete (reduced mortar %passing from 22% to 12%–16%), which is evident through the sieve stability test. These results are influenced by fiber type and percentage.

Table 7
RCPT results found in the literature in comparison with the current study.

Reference	Mix	w/b	Charges Passed (Coulombs)
From [60]	SCC	0.28	340 (Very Low)*
From [61]	SCC	0.35	820 (Very Low)
From [4]	SCC	0.35	535 (Very Low)
Current Study	SCC	0.35	196 (Very Low)
	SFRSCC		251 (Very Low)
	SyFRSCC		131 (Very Low)
	HyFRSCC		598 (Very Low)

* Permeability Class According to ASTM C1202.

Similarly, there was a general improvement in SCC mechanical properties in both phases due to the addition of fibers. The addition of fibers enhanced the overall tensile performance of the SCC matrix, while an extended curing phase through wetting/drying enhanced both compressive strength and modulus of elasticity. Table 8 summarizes the effect of fiber addition on the mechanical properties in both phases. The findings are in good agreement with the properties of FRSCC reported in Table 1. Furthermore, it can be deduced that the fiber addition (steel or synthetic) has negligible effect on the compressive strength and modulus of elasticity of SCC at a Vol.-% dosage of 0.5%.

5.2. Comparison of mechanical properties with ACI equations

The values of the mechanical properties were checked against available formulae included in ACI-318 and ACI-363. A comparison of the test results with the estimated values from both codes was conducted for flexural strength, splitting tensile strength, and modulus of elasticity, and is shown in Fig. 9. Table 9 presents the

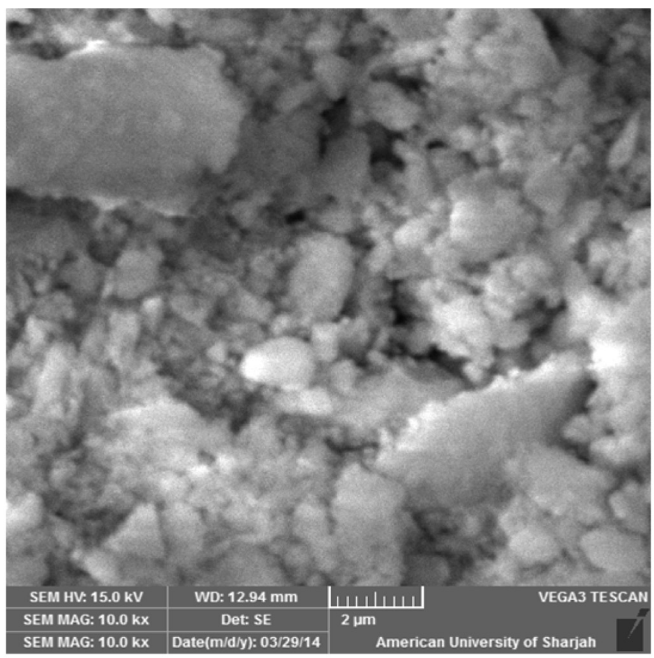

(a) C-S-H plate-like particles

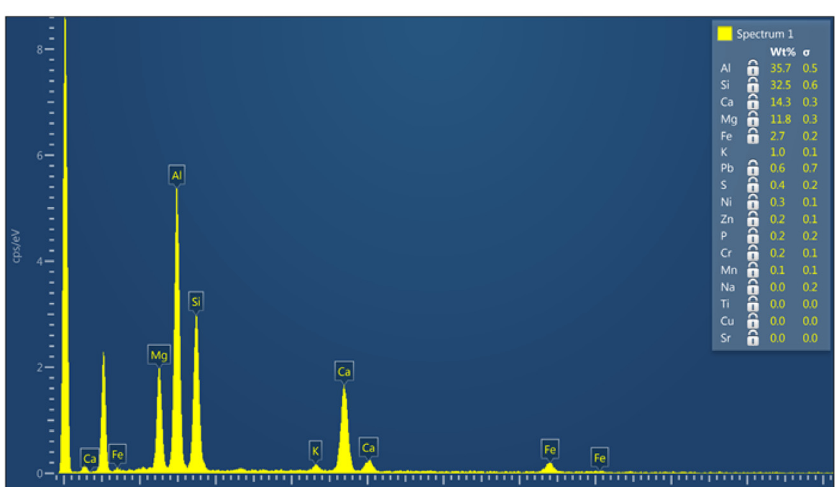

(b) X-ray spectroscopy

Fig. 6. SCC cement morphology (C-S-H).

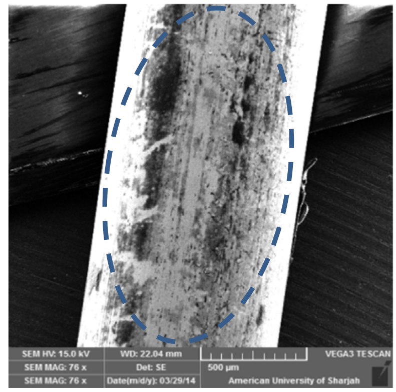

(a) Rough surface texture of steel fiber

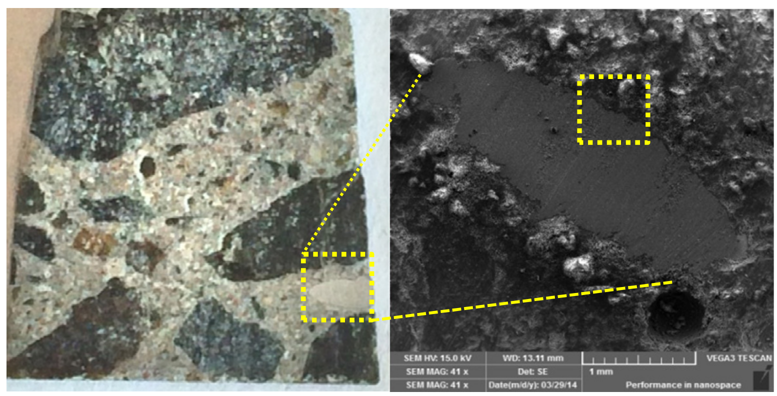

(b) Identified steel fiber to be examined

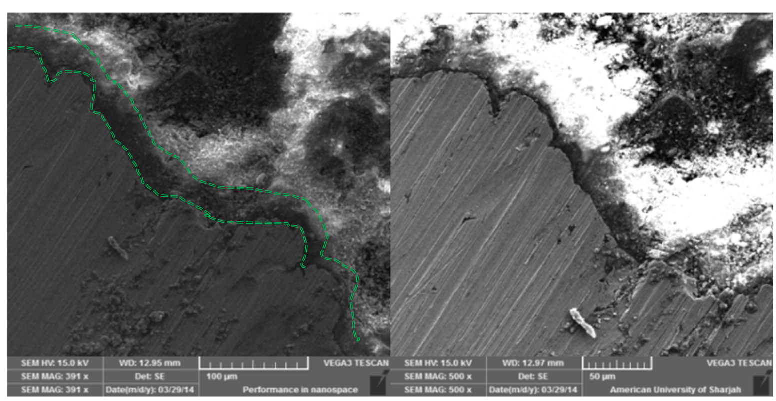

(c) 390X Magn. (d) 500X Magn.

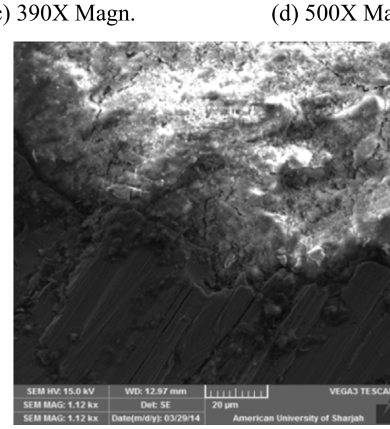

(e) Interaction crack in SFRSCC

Fig. 7. SEM images of SFRSCC sample.

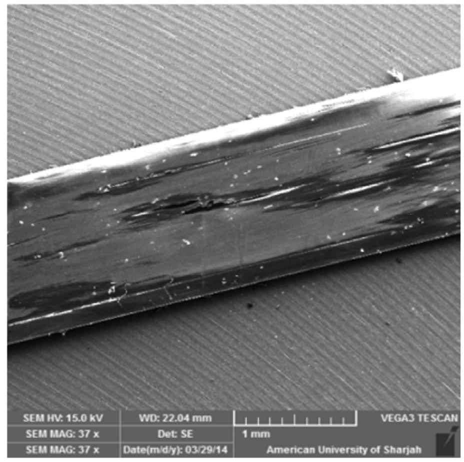

(a) Synthetic fiber filament

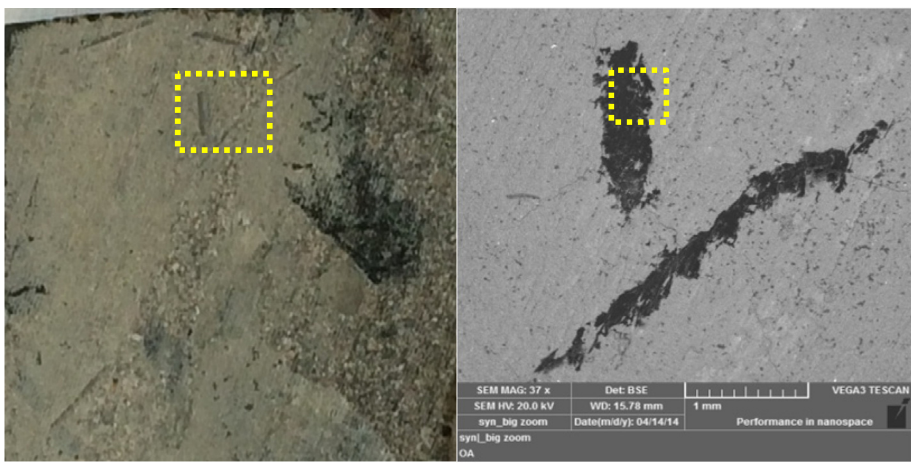

(b) Overall location and identified sample

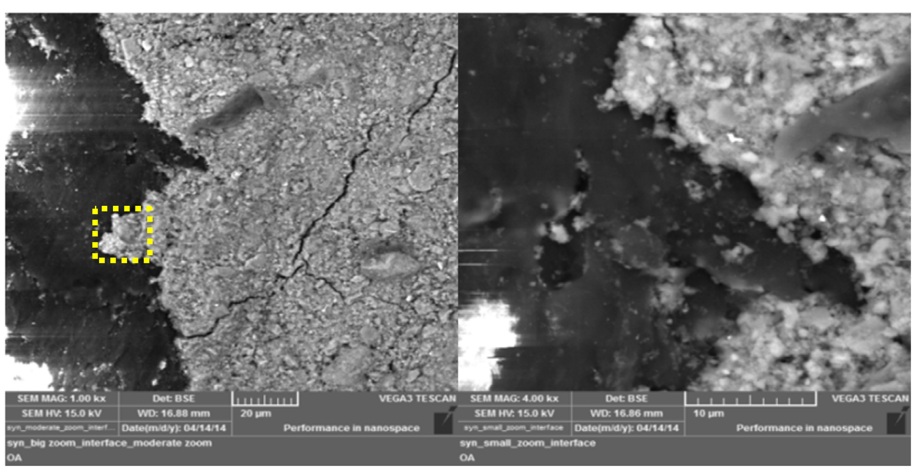

(c) ~1000X Magn. (d) 4000X Magn.

Fig. 8. SEM images of SyFRSCC sample.

list of equations acquired from the ACI-318 and ACI-363 codes, which were used in the analysis and Fig. 9. The limit criteria were predicted for an average cylinder compressive strength of 60 MPa. Overall, the ACI-363 equations provide the closest prediction results to test data.

Modulus of elasticity: Modulus of elasticity values obtained from the current study are significantly lower than the values predicted by both codes as shown in Fig. 9(a). The values obtained from ACI-363 Eq.3 are the closest to the test results. The variation between the test results and the estimated values cannot be linked to the presence of fibers since the control mix has 15% variation from the estimated values already. Meanwhile, the comparison could be affected by the selected type of coarse aggregate used in this study, which is different from the aggregate that ACI equations are based upon; the density of aggregates also affects modulus of elasticity [64]. Although there are some equations in ACI-363 that

Table 8
Summary of FRSCC performance in the current study.

Study Phase	Property		
	Compressive Strength	Flexural and Splitting Tensile Strength	Modulus of Elasticity
Phase I	No significant effect of fibers was observed on ultimate compressive strength. Nevertheless, strength gain rate for SyFRSCC was slower due to water retention at early stages. All FRSCC inhibited explosive failure	Overall increase in flexural and splitting tensile strengths exhibited by all FRSCC mixes. This increase is affected by fiber type and percentage used. However, it was observed that synthetic fibers are more effective at tensile strength improvement due to their dispersion	No significant effect of fibers on elasticity was observed
Phase II	Notable increase in compressive strength of all mixes due to the enhanced hydration process	Overall improvement in tensile properties due to enhanced concrete hydration and fiber inclusion	Slight increase in moduli of elasticity due to increased compressive strength, which is due to an enhanced hydration process

include modification factors to account for the aggregate type, they were evaluated and found to overestimate the modulus of elasticity even more than any of the other equations used in current study. On the other hand, ACI-363 Eq. 3 does not consider the change in properties for SCC and for the influence of fibers on SCC. Nevertheless, the equation provides a good prediction of the modulus of elasticity since it falls around an average value of elasticity moduli obtained from various sources as displayed in (Fig. 9(b)).

Flexural strength: Similar to the modulus of elasticity results, ACI-318 [65] equations overestimate the flexural strength when compared to the equations of ACI-363 [64] as illustrated in Fig. 9(c), indicating the change in mechanical behaviour with the increased compressive strength. ACI-363 Eq. 5 results in the best estimation of the experimental results with only 8% difference with the control samples results. Both SyFRSCC and HyFRSCC mixes showed higher flexural strength than predicted by the code while SFRSCC and control mixes showed lower results than predicted. Nevertheless, the code and the results both support an increase of flexural strengths for all FRSCC mixes. ACI-363 Eq. 5 provides an overall adequate estimate for FRSCC as shown in Fig. 9(d).

Splitting tensile strength: Control, SyFRSCC, and SFRSCC results were all closely estimated by all ACI equations with ACI-363 Eq. 8 being the closest as shown in Fig. 9(e). However, HyFRSCC results were higher in all estimations. This can be explained by the complex composite action of both fibers when combined, in which there is a difference in stiffness between both types of fibers. Results obtained and the predicted values suggest that the fibers improve the splitting tensile strength with steel fibers having a stronger effect. Fig. 9(f) suggests that ACI-363 Eq. 8 is still applicable based on the average statistic values.

The above discussion showed that the ACI equations used in the current study for predicting the modulus of elasticity, flexural strength, and splitting tensile strength provided a very good fit with the experimental results. This indicates that for the 0.5 Vol.-% implemented in this study, the modulus of elasticity, flexural strength, and splitting tensile strength are still governed by the SCC matrix. This means that the equations are applicable for the current volumetric ratio since all mixes achieved similar compressive strengths. This might not be the case for higher volumetric ratios, in which contribution from the fibers on the mechanical properties can be more substantial, rendering the applicability of such equations uncertain.

5.3. Rapid chloride penetration test (RCPT)

While both SFRSCC and HyFRSCC results are in a very low rating, they exhibited higher chloride penetration compared to the control mix. Concerns are raised regarding the application of steel fibers in concrete, due to the high corrosion potential. This can be attributed to the larger cross-sectional area and increased surface friction of steel fibers compared to synthetic fibers. SFRSCC and

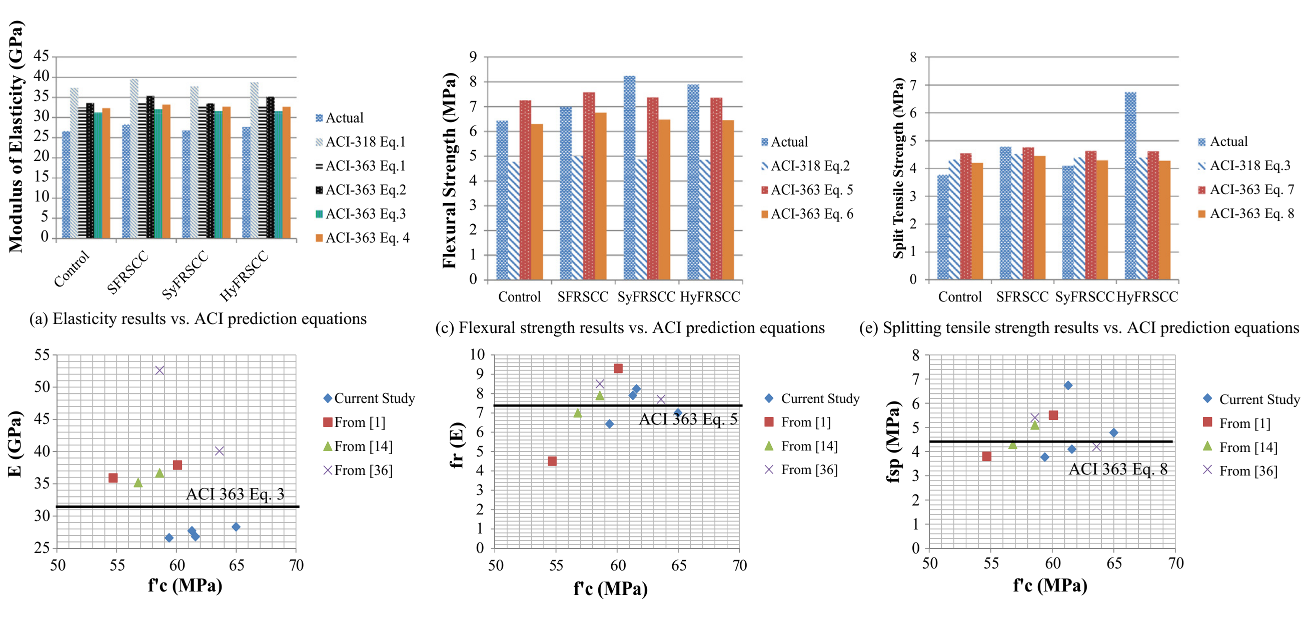

Fig. 9. Comparison of FRSCC mechanical properties vs. ACI prediction equations.

Table 9
ACI equations used for comparison with results from the current study.

Property	Label	Equation
Modulus of Elasticity (E_c) (GPa)	ACI 318 Eq. 1	$E_c = 0.043 w_c^{1.5}\sqrt{f'_c}$
	ACI 363 Eq. 1	$E_c = 3320\sqrt{f'_c} + 6900$
		for 21 MPa $< f'_c <$ 83 MPa
	ACI 363 Eq. 2	$E_c = 3.385 \times 10^{-5} w_c^{2.5} f_c'^{0.325}$
		for $f'_c <$ 84 MPa
	ACI 363 Eq. 3	$E_c = 14495 + 2176\sqrt{f'_c}$
	ACI 363 Eq. 4	$E_c = 9500 f_c'^{0.3}$
		for 25 MPa $< f'_c <$ 85 MPa
Flexural Strength (f_r) (MPa)	ACI 318 Eq. 2	$f_r = 0.62\lambda\sqrt{f'_c}$
	ACI 363 Eq. 5	$f_r = 0.94\sqrt{f'_c}$
		for 21 MPa $< f'_c <$ 83 MPa
	ACI 363 Eq. 6	$f_r = 0.25 f_c'^{0.79}$
		for moist and steam cured
Splitting Tensile Strength (f_{sp}) (MPa)	ACI 318 Eq. 3	$f_{sp} = 0.56\sqrt{f'_c}$
	ACI 363 Eq. 7	$f_{sp} = 0.59\sqrt{f'_c}$
		for 21 MPa $< f'_c <$ 83 MPa
	ACI 363 Eq. 8	$f_{sp} = 0.32 f_c'^{0.63}$

Note: w_c: unit weight of concrete (kg/m^3), f'_c: cylinder compressive strength (MPa), λ: modification factor for lightweight concrete

HyFRSCC samples showed sign of corrosion (indicated by rust formation); nevertheless, such corrosion can occur locally on the surface of concrete and there is no evidence of its propagation deeper into concrete. Regardless of compaction and workability of the concrete, fibers will always remain in the concrete cover, and they can corrode, creating brownish spots on the surface [66]. By inspecting the RCP tested specimens of the SFRSCC mix, such rust formation occurred only on the surface of the tested sample in the current study. As for HyFRSCC, the interaction between steel and synthetic fiber increased the permeability of concrete relative to the control mix, despite achieving a very low penetration potential which is determined according to ASTM C1202. This is associated with the expected increase of internal voids in zones of interaction between steel and synthetic fibers. On the other hand, SyFRSCC exhibited the lowest RCP value, indicating a significant reduction in permeability relative to the control mix. This is mainly attributed to the small diameter of the fibers [67].

5.4. Scanning Electron Microscopy

From the SEM images of FRSCC, it was observed that the mix proportioning and packing of particles led to a dense microstructure. The micro-particle size distribution of C-S-H (hydration product) resulted in a high level of density, which is indicated by the very low potential of chloride ion penetration from the RCP test results for all mixes. Nevertheless, the ITZ of SyFRSCC and SFRSCC mixes was different between synthetic and steel fibers concerning crack initiation/propagation resistance. As is shown in Fig. 7(b), the constricted interlock increases the stiffness/strength of the bond between surrounding mortar and fibers. Although this interlock exists in both mixes, the surface roughness and angularity of steel fibers' surface differs than that of synthetic fibers [68]. Such constriction increases the energy/load required to fracture (crack) the material [29]. This explains why steel fibers can resist macrocracking [15]. Moreover, ductility/load resistance gained from the addition of the steel fibers relies more on the slippage/anchorage of the fibers in concrete. On the other hand, although having a lower bond strength with concrete, synthetic fibers tend to locally act as reinforcement through anchorage and confinement. However synthetic fibers, more commonly, fail in shear (higher stress level) rather than debonding from concrete regardless of the mix design, as depicted in Fig. 5. Such mechanism is attainable due to the high dispersion ability, geometry, and large surface area. Therefore, this mechanism is beneficial for the overall macro properties of concrete, because this will increase the energy dissipation capacity and improves the ductile behaviour. Equally important, the addition of fibers, especially steel, introduces micro-cracking in SCC, which was discussed also by [41]. This is due to the relative difference in stiffness between the components (fiber, mortar, aggregates). Tensile stresses develop during hydration, and micro-cracks will radially emerge between aggregates and fibers through the mortar, as opposed to tangential cracking which implies improper FRSCC quality. Nonetheless, such effect should not be considered a shortcoming, particularly that the addition of fibers enhances the chloride penetration resistance of concrete and other mechanical properties. Thus, it is believed that strength is highly determined by the amount of water, water transport, and the effective w/b ratio present in the matrix, without being affected by the presence of fibers [31,44]. From the SEM images, it was shown that a wall-effect was present in the ITZ of SFRSCC, while there was a good ITZ in SyFRSCC. Since steel fibers cannot absorb water, physical and physical-chemical forces can be the main reason for attracting non-chemically bound water [69]. Such forces include electrostatic, magnetic, and Van der Waal forces. Throughout hydration, water is consumed during the chemical reaction forming C-S-H. On the other hand, synthetic fibers reduce the capillarity of concrete, and block possible pathways for water evaporation or loss into the atmosphere, retaining water inside the matrix, especially with proper curing [67]. This is due to the physical entrapment of water particles in contact since synthetic fibers are also non-absorptive by nature. Therefore, the lower early strength gain is mainly due to the delayed hydration process. Contrary to steel fibers, synthetic fibers do not possess magnetic or electrostatic forces that can resist capillary water transport due to hydration from neighboring cement particles, allowing them to fully hydrate. This leads not only to attain similar strength of a reference mixture, but also to a higher strength due to the water retention.

6. Conclusions

In this paper, the behaviour of FRSCC concerning mechanical and durability properties was investigated. The main conclusions drawn from this study are:

- All mixes containing fibers achieved adequate flowability, filling ability, and segregation resistance. Nonetheless, synthetic fibers reduced the passing ability of SCC more than steel fiber. This is attributed to the higher surface area and aspect ratio of synthetic fibers compared to steel fibers at a similar volumetric ratio.

- Fibers had a negligible effect on the compressive strength and modulus of elasticity of SCC. The flexural and splitting tensile strengths of all FRSCC were higher than that of the control mixture by 7%–26% and 12%–79%, respectively confirming the positive effect of fibers on counteracting the propagation of macro-cracks and restraining micro-cracks. The modulus of elasticity of FRSCC was not significantly affected. However, an improvement in the post-cracking behaviour of all FRSCC until failure was observed.
- Findings of the current study were in a close range with the estimated results of the equations in ACI. The ACI equations used in the current study for estimating the modulus of elasticity, flexural strength, and splitting tensile strength are governed by the concrete matrix/type rather than being influenced by the fibers at 0.5 Vol.-%
- Subjecting FRSCC to wet and dry cycles for 21 days provided an improved hydration process. An enhanced performance in terms of compressive strength, flexural strength, splitting tensile strength, and modulus of elasticity, was achieved compared to specimens in a controlled environment.
- All mixes presented low chloride permeability when tested in RCPT confirming an adequate durability of SCC and FRSCC. This was attributed to the high density of the mix, even at a microstructural level.
- The microstructure and ITZ depended on the mixture composition. Steel fiber exhibited a wall effect with the surrounding cement paste, while synthetic fiber did not. For both fiber types, there was some interlock observed with the surrounding mortar, with a more pronounced interlock observed between concrete and steel fibers.
- Due to the higher stiffness of steel fibers compared to the cement paste, tensile micro-cracks initiated during hydration.

Acknowledgments

This research effort was financially supported by the American University of Sharjah Provost's Challenge (Grant no. FRG11-1). The contribution of Mr. Saleh Chalbi and Mr. Majed Touqan during the experimental program is highly appreciated.

References

[1] O. Gencel, W. Brostow, T. Datashvili, M. Thedford, Workability and mechanical performance of steel fiber-reinforced self-compacting concrete with fly ash, Compos. Interfaces 18 (2) (2011) 169–184.
[2] K.M.A. Hossain, M. Lachemi, Fresh, mechanical, and durability characteristics of self-consolidating concrete incorporating volcanic ash, ASCE J. Mater. Civil Eng. 22 (7) (2010) 651–657.
[3] H. Mazaheripou, S. Ghanbarpour, S.H. Mirmoradi, I. Hosseinpour, The effect of polypropylene fibers on the properties of fresh and hardened lightweight self-compacting concrete, Constr. Build. Mater. 251 (1) (2011) 351–358.
[4] S.D. Hwang, K. Khayat, Durability characteristics of self-consolidating concrete designated for repair applications, Mater. Struct. 42 (1) (2009) 1–14.
[5] A.L. Ardeshana, A.K. Desai, Durability of fiber reinforced concrete of marine structures, Int. J. Eng. Res. Appl. 4 (2) (2012) 215–219.
[6] S. Cattaneo, F. Giussani, F. Mola, Flexural behaviour of reinforced, prestressed and composite self-consolidating concrete beams, Constr. Build. Mater. 36 (11) (2012) 826–837.
[7] L. Ferrara, Y.D. Park, S.P. Shah, A method for mix-design of fiber-reinforced self-compacting concrete, Cem. Concr. Res. 37 (6) (2007) 957–971.
[8] V. Corinaldesi, G. Moriconi, Characterization of self-compacting concretes prepared with different fibers and mineral additions, Cement Concr. Compos. 33 (5) (2011) 596–601.
[9] A.C. Aydin, Self compactability of high volume hybrid fiber reinforced concrete, Constr. Build. Mater. 21 (6) (2007) 1149–1154.
[10] M. Sahmaran, A. Yurtseven, O. Yaman, Workability of hybrid fiber reinforced self-compacting concrete, Build. Environ. 40 (12) (2005) 672–1677.
[11] W. Khaliq, V.K.R. Kodur, Effect of high temperature on tensile strength of different types of high-strength concrete, ACI Mater. J. 108 (4) (2011) 394–402.
[12] K.K. Sideres, P. Manita, Residual mechanical characteristics and spalling resistance of fiber reinforced self-compacting concretes exposed to elevated temperatures, Constr. Build. Mater. 41 (4) (2013) 296–302.
[13] F. Pelisser, A.B.D.S.S. Neto, H.L. La Rovere, R.C.D.A. Pinto, Effect of the addition of synthetic fibers to concrete thin slabs on plastic shrinkage cracking, Constr. Build. Mater. 24 (11) (2010) 2171–2176.
[14] O. Gencel, C. Ozel, C. Brostow, G. Martínez-Barrera, Mechanical properties of self-compacting concrete reinforced with polypropylene fibres, Mater. Res. Innovations 15 (3) (2011) 216–225.
[15] B. Akcay, M.A. Tasdemir, Mechanical behaviour and fibre dispersion of hybrid steel fibre reinforced self-compacting concrete, Constr. Build. Mater. 28 (1) (2012) 287–293.
[16] ACI 544.1, State-of-the-Art Report on Fiber Reinforced Concrete, American Concrete Institute, Farmington Hills, Michigan, USA, 2009.
[17] M.C. Brown, H.C. Ozyildirim, W.L. Duke, Investigation of steel and polymer fiber-reinforced self-consolidating concrete, ACI Mater. J. 274 (2010) 69–78.
[18] P.L. Domone, A review of the hardened mechanical properties of self-compacting concrete, Cement Concr. Compos. 29 (1) (2007) 1–12.
[19] D. Forgeron, A. Omer, Flow characteristics of macro-synthetic fiber-reinforced concrete, ACI Mater. J. 274 (2010) 1–14.
[20] S. Yazici, G. Inan, V. Tabak, Effect of aspect ratio and volume fraction of steel fiber on the mechanical properties of SFRC, Constr. Build. Mater. 21 (6) (2007) 1250–1253.
[21] B.W. Xu, H.S. Shi, Correlations among mechanical properties of steel fiber reinforced concrete, Constr. Build. Mater. 23 (12) (2009) 3468–3474.
[22] S. Yehia, Evaluation of steel fiber distribution in a concrete matrix, in: Concrete Repair, Rehabilitation and Retrofitting III: 3rd International Conference on Concrete Repair, Cape Town, South Africa, 2012.
[23] L. Cominoli, C. Failla, G.A. Plizzari, Steel and synthetic fibres for enhancing concrete toughness and shrinkage behavior, in: International Conference on Sustainable construction materials and technologies, Coventry, UK, 2007, pp. 231–240.
[24] J. Tao, Y. Yuan, L. Taerwe, Compressive strength of self-compacting concrete during high-temperature exposure, ASCE J. Mater. Civil Eng. 22 (10) (2010) 1005–1011.
[25] Y. Ding, Y. Zhang, A. Thomas, The investigation on strength and flexural toughness of fibre cocktail reinforced self-compacting high performance concrete, Constr. Build. Mater. 23 (1) (2009) 448–452.
[26] B. Boulekbache, M. Hamrat, M. Chemrouk, S. Amziane, Influence of yield stress and compressive strength on direct shear behaviour of steel fibre-reinforced concrete, Constr. Build. Mater. 27 (1) (2012) 6–14.
[27] S. Yehia, O. Abudayyeh, O. Bhusan, M. Maurovich, A. Zalt, Self-consolidating concrete mixture with local materials: proportioning and evaluation, Mater. Sci. Res. J. 3 (1–2) (2009) 41–64.
[28] K. Hossain, M. Lachemi, M. Sammour, M. Sonebi, Influence of polyvinyl alcohol, steel, and hybrid fibers on fresh and rheological properties of self-consolidating concrete, ASCE J. Mater. Civil Eng. 24 (9) (2012) 1211–1220.
[29] N. Buratti, C. Mazzotti, M. Savoia, Post-cracking behaviour of steel and macro-synthetic fibre-reinforced concretes, Constr. Build. Mater. 25 (5) (2011) 2713–2722.
[30] M. Hsie, C. Tu, P.S. Song, Mechanical properties of polypropylene hybrid fiber-reinforced concrete, Mater. Sci. Eng., A 494 (1–2) (2008) 153–157.
[31] S. Erdem, A.R. Dawson, N.H. Thom, Microstructure-linked strength properties and impact response of conventional and recycled concrete reinforced with steel and synthetic macro fibres, Constr. Build. Mater. 25 (10) (2011) 4025–4036.
[32] A. Lanzoni, A. Nobili, A.M. Tarantino, Performance evaluation of a polypropylene-based draw-wired fibre for concrete structures, Constr. Build. Mater. 28 (1) (2012) 798–806.
[33] S. Grunewald, J.C. Walraven, Maximum fiber content and passing ability of self-consolidating fiber-reinforced concrete, ACI Mater. J. 274 (2010) 15–29.
[34] W. Labib, N. Eden, Report on an Investigation into the Use of Fibres in Concrete Industrial Ground-Floor Slabs, University of Liverpool, 2006.
[35] G. Khalaj, A. Nazari, Modeling split tensile strength of high strength self-compacting concrete incorporating randomly oriented steel fibers and SiO_2, Compos. B Eng. 43 (4) (2012) 1887–1892.
[36] E.T. Dawood, M. Ramli, Mechanical properties of high strength flowing concrete with hybrid fibers, Constr. Build. Mater. 28 (1) (2012) 193–200. 2012.
[37] M. Sahmaran, I.O. Yaman, Hybrid fiber reinforced self-compacting concrete with a high-volume coarse fly ash, Constr. Build. Mater. 21 (1) (2007) 150–156.
[38] J. Roesler, D. Lange, S. Altoubat, K. Rieder, G. Ulreich, Fracture of plain and fiber-reinforced concrete slabs under monotonic loading, ASCE J. Mater. Civil Eng. 16 (2004) 452–460 (Special Issue).
[39] S. Altoubat, A. Yazdanbakhsh, K.A. Rieder, Shear behavior of macro-synthetic fiber-reinforced concrete beams without stirrups, ACI Mater. J. 106 (4) (2009) 381–389.
[40] V.M.C.F. Cunha, J.A.O. Barros, J.M. Sena-Cruz, Tensile behavior of steel fiber reinforced self-compacting concrete, ACI Mater. J. 274 (2010) 51–68.
[41] A.S. El-Dieb, Mechanical, durability and microstructural characteristics of ultra-high-strength self-compacting concrete incorporating steel fibers, Mater. Des. 30 (10) (2009) 4286–4292.
[42] S. Yehia, M. AlHamaydeh, S. Farrag, High strength lightweight SCC matrix with partial normal weight coarse aggregate replacement: strength and durability evaluations, ASCE J. Mater. Civil Eng. 26 (11) (2014).
[43] S. Ahmad, A.K. Azad, Hameed M. Abdul, A study of self-compacting concrete made with marginal aggregates, Arab. J. Sci. Eng. 33 (2B) (2008) 437–442.
[44] A.M. Neville, Properties of Concrete, fourth ed., John Wiley & Sons Inc., New York, 1996.

[45] EFNARC, Specification and Guidelines for Self-Compacting Concrete 2002, The European Federation of Specialist Construction Chemicals and Concrete Systems.
[46] BS 12390-3, Testing Hardened Concrete: Compressive Strength of Test Specimens, British Standard Institute, London UK, 2009.
[47] ASTM C39, Standard Test Method for Compressive Strength of Cylindrical Concrete Specimens, ASTM International, West Conshohocken, PA, 2014.
[48] ASTM C496/C496M, Standard Test Method for Splitting Tensile Strength of Cylindrical Concrete Specimens, ASTM International, West Conshohocken, PA, 2011.
[49] ASTM C78/C78M, Standard Test Method for Flexural Strength of Concrete Using Simple Beam with Third-Point Loading, ASTM International, West Conshohocken, PA, 2010.
[50] ASTM C469/C469M, Standard Test Method for Static Modulus of Elasticity and Poisson's Ratio of Concrete in Compression, ASTM International, West Conshohocken, PA, 2010.
[51] ASTM C1202, Standard Test Method for Electrical Indication of Concrete's Ability to Resist Chloride Ion Penetration, ASTM International, West Conshohocken, PA.
[52] BEKAERT, DRAMIX 65/60 Product Data Sheet, 2005 (Retrieved on April 7th, 2014).
[53] GRACE Construction Products, STRUX 90/40 – Synthetic Macro Fiber Reinforcement, 2007 (Retrieved on April 7th, 2014).
[54] BS 933-3:2012, Tests for Geometrical Properties of Aggregates. Determination of Particle Shape: Flakiness Index, British Standards Institute, London UK, 2012.
[55] BS 812-105.2, Method for Determination of Particle Size: Elongation Index of Coarse Aggregate, British Standards Institute, London UK, 1990.
[56] ASTM C29/29M, Standard Test Method for Bulk Density (Unit Weight) and Voids in Aggregate, ASTM International, West Conshohocken, PA, 2009.
[57] ASTM C127, Standard Test Method for Density, Relative Density (Specific Gravity), and Absorption of Coarse Aggregate, ASTM International, West Conshohocken, PA, 2012.
[58] BS 1097-2, Tests for Mechanical and Physical Properties of Aggregates: Methods for the Determination of Resistance to Fragmentation, British Standards Institute, London UK, 2010.
[59] ASTM C131, Standard Test Method for Resistance to Degradation of Small-Size Coarse Aggregate by Abrasion and Impact in the Los Angeles Machine, ASTM International, West Conshohocken, PA, 2006.
[60] G. Nayak, M.C. Narasimhan, S.V. Rajeeva, Chloride-ion impermeability of self-compacting high-volume fly ash concrete mixes, Int. J. Civ. Environ. Eng. 11 (4) (2011) 29–35.
[61] K.M.A. Hossain, M. Lachemi, Characteristics of self-consolidating concrete incorporating volcanic ash, in: 32nd Conference on Our World in Concrete & Structures, Singapore, 2007.
[62] K. Ravi, K.B. Prakash, Strength characteristics of hybrid fiber reinforced self compacting concrete subjected to sustained elevated temperature, in: Presented at the 33rd Our World in Concrete & Structures, Singapore, 2008.
[63] S. Tarun, G. Sanjay, B. Manish, Workability and compressive strength of steel polypropylene hybrid fibre reinforced self-compacting concrete, Int. J. Sci. Emerg. Technol. Latest Trends 6 (2013) 7–13.
[64] ACI-318, Building Code Requirements for Structural Concrete and Commentary, American Concrete Institute, Farmington Hill, Michigan, 2011.
[65] ACI-363R, Report on High-Strength Concrete, American Concrete Institute Farmington Hills, Michigan, 2010.
[66] S.U. Balouch, J.P. Forth, J.L. Granju, Surface corrosion of steel fibre reinforced concrete, Cem. Concr. Res. 40 (3) (2010) 410–414.
[67] H. Bolat, O. Simsek, M. Cullu, G. Durmus, O. Can, The effects of macro synthetic fiber reinforcement use on physical and mechanical properties of concrete, Compos. B 61 (5) (2014) 191–198.
[68] L. Yan, R.L.P. Pendleton, C.H.M. Jenkins, Interface morphologies in polyolefin fiber reinforced concrete composites, Compos. A 29 (5–6) (1998) 643–650.
[69] R. Cerny, P. Rovnanikova, Transport Processes in Concrete, first ed., Spon Press, New York, USA, 2002.